Universal gene co-expression network reveals receptor-like protein genes conferring broad-spectrum resistance in pepper (*Capsicum annuum* L.)

Running title: conserved CaRLPs in GCN conferring broad-spectrum resistance

Won-Hee Kang[1]*, Junesung Lee[2], Namjin Koo[3], Ji-Su Kwon[2], Boseul Park[2], Yong-Min Kim[3,4], Seon-In Yeom[1,2]*

[1] Institute of Agriculture & Life Science, Gyeongsang National University, Jinju, 52828, Republic of Korea

[2] Department of Horticulture, Division of Applied Life Science (BK21 four), Gyeongsang National University, Jinju, 52828, Republic of Korea

[3] Korean Bioinformation Center, Korea Research Institute of Bioscience and Biotechnology, Daejeon, 34141, Republic of Korea

[4] Genome Engineering Research Center, Korea Research Institute of Bioscience and Biotechnology, Daejeon, 34141, Republic of Korea

*Corresponding author:

Seon-In Yeom (E-mail: sunin78@gnu.ac.kr)

Won-Hee Kang (E-mail: wh81kang@gmail.com)

ABSTRACT

Receptor-like proteins (RLPs) on the plant cell surface have been implicated in immune responses and developmental processes. Although hundreds of *RLP* genes have been identified in plants, only a few RLPs have been functionally characterized in a limited number of plant species. Here, we identified *RLPs* in the pepper (*Capsicum annuum*) genome, and performed comparative transcriptomics coupled with the analysis of conserved gene co-expression networks (GCNs) to reveal the role of core RLP regulators in pepper–pathogen interactions. A total of 102 RNA-seq datasets of pepper plants infected with four pathogens were used to construct CaRLP-targeted GCNs (CaRLP-GCN). All resistance-responsive CaRLP-GCNs were merged to construct a universal GCN. Fourteen hub *CaRLPs*, tightly connected with defense related gene clusters, were identified in eight modules. Based on the CaRLP-GCNs, we experimentally tested whether hub *CaRLPs* in the universal GCN are involved in biotic stress response. Of the nine hub *CaRLPs* tested by virus-induced gene silencing (VIGS), three genes (*CaRLP264*, *CaRLP277*, and *CaRLP351*) showed defense suppression with less hypersensitive response (HR)-like cell death in race-specific and non-host resistance response to viruses and bacteria, respectively, and consistently enhanced susceptibility to *Ralstonia solanacearum* and/or *Phytophthora capsici*. These data suggest that key *CaRLPs* exhibit conserved functions in response to multiple biotic stresses and can be used for engineering of a plant with broad-spectrum resistance. Altogether, we show that generation of a universal GCN using comprehensive transcriptome datasets could provide important clues for uncovering genes involved in various biological processes.

INTRODUCTION

Plants employ extra- and intracellular immune signaling to protect themselves against pathogens[1,2]. The first layer of plant immunity, known as pattern-triggered immunity, is activated upon the perception of pathogen- or microbe-associated molecular patterns (PAMPs or MAMPs) by plant cell surface-localized pattern recognition receptors (PRRs). PRRs sense diverse pathogens including bacteria, fungi, oomycetes and parasitic plants, and are involved in the immune signaling complex and network[3]. Recently, plant PRRs have been successfully used to confer broad-spectrum resistance in potato (*Solanum tuberosum*)[4,5] and in *Nicotiana benthamiana* and tomato (*Solanum lycopersicum*) (Lacombe et al., 2010), and have been considered for conferring broad-spectrum disease resistance in other crops.

Plant PRRs are distinguished into two main classes, depending on their cytoplasmic kinase domains: receptor-like kinases (RLKs) and receptor-like proteins (RLPs). RLKs contain an extracellular domain, a single transmembrane domain and a cytoplasmic domain, whereas RLPs lack the cytoplasmic kinase domain but carry a short cytoplasmic tail. RLPs play crucial roles in plant immunity against pathogens. The first RLPs, designated as *Cf* genes, were identified in tomato, which imparted resistance to *Cladosporium fulvum* isolates[6-9]. Since then, several RLPs have been shown to have function in plant defense, mostly in Solanaceous plants and *Arabidopsis thaliana*[5,10-18]. In addition, RLPs are also involved in plant development [19-21]. A number of genes encoding RLPs have been identified with the completion of plant genome project[22-27]; however, relatively fewer genes have been functionally characterized to date.

Based on the recent advances in the sequencing technology, along with the decline in the cost of sequencing, RNA-seq have been widely utilized in plants, producing massive amounts of data. However, the identification and manipulation of information of interest from large integrated datasets remain challenging. Since functionally associated genes often show transcriptional co-regulation, gene co-expression networks (GCNs) present an important resource for the identification of novel genes within a given biological process-regulating module. Thus, the analysis of GCNs could be a powerful approach for predicting gene functions and isolating modules involved in specific biological process across large-scale gene expression data[28-31]. In recent years, GCN analysis has been successfully used to discover stress-responsive genes in plants[32-34]. Additionally, several research groups recently performed comparative and combined analyses of GCNs in time-series experiments conducted under various conditions and with multiple treatments, across different species and kingdoms[35-39]. These studies were used to identify hub genes and infer their roles in

79 biological processes. However, that are less well investigated compared with certain model
80 species because of their extreme complexity and limited resources.

81 Chili pepper (*Capsicum* spp.), a member of the Solanaceae family, is an important
82 vegetable crop worldwide. However, pepper production is threatened by pathogens such as
83 fungi, bacteria, viruses, insects, and nematodes. Development of pathogen resistant
84 cultivars is one of the best approaches for controlling infection in pepper. Although multiple
85 reference genomes and transcriptome datasets of pepper have been published recently[40-43],
86 the molecular mechanism underlying plant immunity remains unclear. Therefore, the
87 identification and characterization of genes involved in plant defense using comprehensive
88 transcriptome data is critical. In this study, we identified 438 RLP genes in the chili pepper
89 genome through phylogenetic analysis and comparative transcriptomic analysis of 102 RNA-
90 seq datasets of chili pepper plants challenged with four different pathogens. In addition, we
91 constructed CaRLP-targeted GCNs (CaRLP-GCN) using comprehensive RNA-seq datasets
92 and, merged the resistant-responsive GCNs to develop a universal CaRLP-GCN. Using this
93 GCN, we identified 14 putative RLP hub genes belonging to eight modules. Loss-of-function
94 analysis of three *CaRLPs* (*CaRLP264*, *CaRLP277*, and *CaRLP351*) validated the broad
95 immune response to pathogens. The silencing of each of the three *CaRLPs* significantly
96 reduced the broad-spectrum resistance against viruses, bacteria, and oomycetes. Overall,
97 this study demonstrates the successful characterization of novel genes via the construction
98 of a universal GCN from large RNA-seq datasets, and provides key insights into the broad-
99 spectrum resistance in plants.

100

101

RESULTS

Genome-wide identification and classification of RLPs in pepper genome

A total of 438 RLP-encoding genes were identified in the *Capsicum annuum* genome by excluding redundant sequences and genes encoding NB-ARC or kinase domain-containing proteins, and by validating the RLP structure (see Materials and Methods for details). All of the RLP-encoding genes were renamed according to their chromosomal positions (Fig. 1a and Supplementary Table S1). Details of *CaRLP* genes are summarized in Supplementary Table S1.

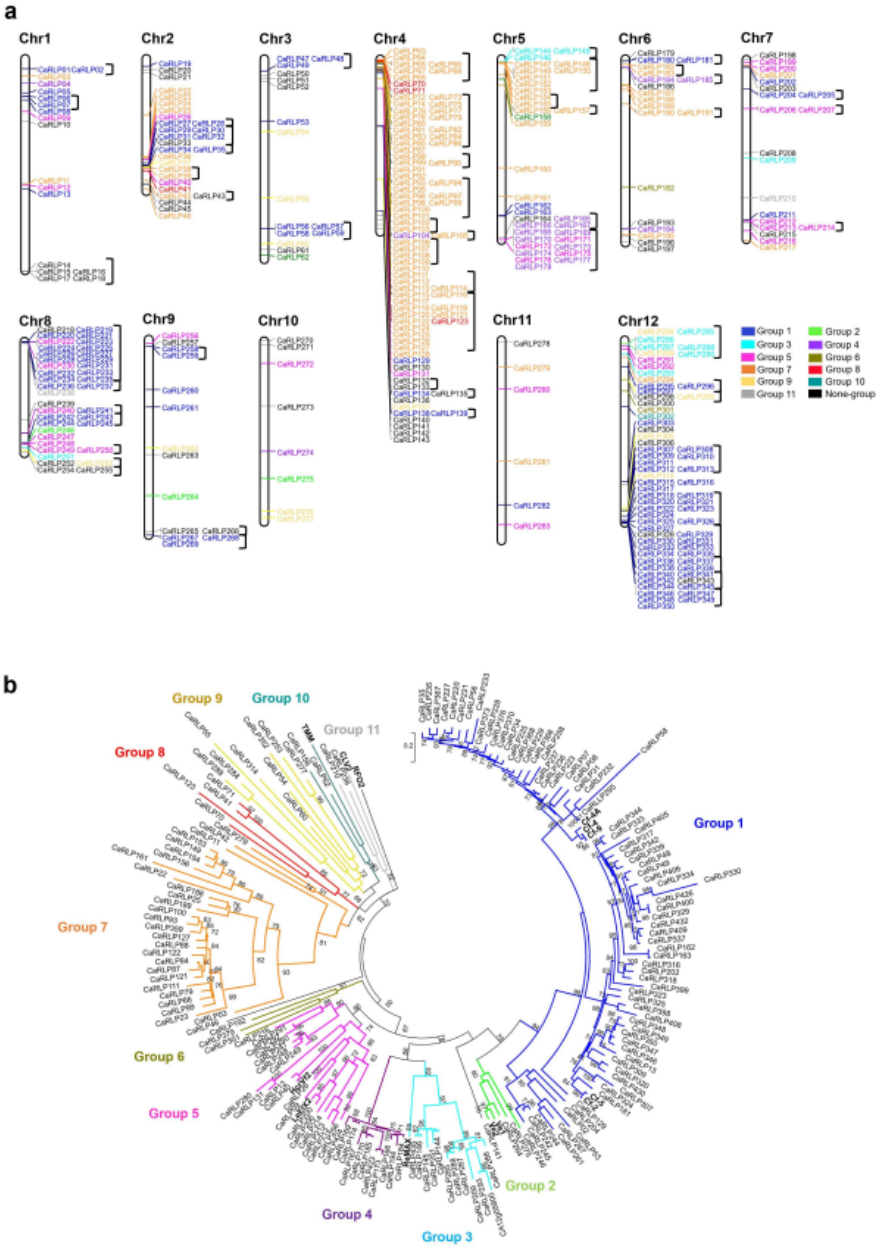

Fig. 1. Phylogenetic analysis and chromosomal locations of *CaRLPs*. (a) Physical location of *CaRLP* genes on pepper chromosomes. A total of 350 *CaRLPs* were located on 12 chromosomes, while 88 *CaRLPs* were assigned to pepper scaffolds. The chromosome and scaffold numbers are indicated at the top of each chromosome. *CaRLPs* are colored according to their phylogenetic group. Black square brackets on the right side of gene IDs indicate the physical gene clusters of CaRLPs on chromosomes**.** (b) Phylogenetic tree of CaRLPs constructed using the maximum-likelihood method using PhyML. Bootstrap values over 60 are indicated above branches. Clades containing known *RLP* genes are indicated by the *RLP* gene names at the end of the clade.

Phylogenetic analysis and sequence similarity-based clustering methods[24,44] classified 364 out of 438 CaRLPs into 11 groups; the remaining 74 CaRLPs were not classified into any group and were defined as singletons (Fig. 1b and Supplementary Table S1). The majority of RLPs were assigned to two groups (1 and 7). Group 1 was the largest group consisting of comprising 153 genes, including tomato *SlCf* genes and their homologs in pepper. Group 7 was the second largest group comprising 118 *CaRLP* genes, without known genes. Next, to explore the evolutionary relationships of CaRLPs with SlRLPs[24] and AtRLPs[22], we conducted phylogenetic analysis of the amino acid sequence of conserved C3-D domain of these RLPs (Supplementary Fig. S1). The majority of CaRLPs clustered together with SlRLPs, whereas most of the AtRLPs grouped separately, forming two Arabidopsis-specific clades (Supplementary Fig. S1). These results suggest that the *CaRLP* gene family underwent expansion after divergence from the common ancestor of Arabidopsis and Solanaceae species.

Chromosomal location, physical cluster, and conserved motif analyses

Of the 438 *CaRLP* genes identified in this study, 350 mapped on to 12 chromosomes, while 88 were assigned to unmapped scaffolds (Fig. 1a). Most of the *CaRLPs* belonging to the same phylogenetic group were closely clustered on a given chromosome. Next, we performed physical cluster analysis to thoroughly investigate the chromosomal distribution of *CaRLPs*. The results revealed 54 clusters on pepper chromosomes containing 227 genes (Fig. 1a and Supplementary Table S2). Each of these clusters spanned a physical distance of 0.7–885 kb. Large clusters (>200 kb) were located on chromosomes 1, 4, 5, 8, and 12, and no cluster was identified on chromosomes 10 and 11. Of all the *CaRLPs* in each group, those with large numbers (Groups 1 and 7) formed mostly physical clusters. To better understand the *CaRLP* gene family, we examined conserved motifs in CaRLP proteins. A total of 20 distinct motifs were predicted among all

438 CaRLPs and known RLPs (Fig. S2 and Supplementary Table S3). Most motifs were found to encode the leucine-rich repeat (LRR) domain, while motif 9 encoded the transmembrane region. Most of the closely related genes in the same phylogenetic group exhibited common motif compositions. Taken together, these data indicate that CaRLPs belonging to the same phylogenetic group share conserved motifs, similar protein domain compositions and similar chromosomal locations.

Expression analysis of *CaRLPs* in response to biotic stresses

RLPs perform crucial roles in plant disease resistance. However, little is known about the possible function of CaRLPs in defense response. To further understand the role of *CaRLP* genes in plant defense, we investigated the expression patterns of *CaRLPs* showing differential expression between uninoculated (control) and pathogen-challenged pepper plants; these genes are hereafter referred to as differentially expressed *CaRLP* genes (*CaRLP*-DEGs). These DEGs were obtained from 63 previously published RNA-seq datasets of pepper plants infected with three different viruses including *Tobacco mosaic virus* (TMV) pathotype P0 (TMV-P0), TMV pathotype P2 (TMV-P2) and *Pepper mottle virus* (PepMoV)[43,45]. In addition, to determine the changes in *CaRLP* expression at an early stage of oomycete infection, we generated six-timepoint RNA-seq datasets from three biological replicates of *P. capsici*-inoculated and control pepper plants (Supplementary Table S4). Thus, we examined a total of 102 RNA-seq datasets to analyze the expression of *CaRLPs* (Supplementary Table S5). Pepper accession 'CM334,' which was used for RNA-seq analysis in this study, is known to be resistant to TMV-P0, PepMoV, and *P. capsici* but susceptible to TMV-P2[45,46].

Of the 438 *CaRLPs*, 35 were differentially expressed between TMV-P0-inoculated and control plants, and 6 were differentially expressed between PepMoV-inoculated and control plants (fold-change ≥ 2) at one or more time points (Supplementary Fig. S3, and Supplementary Table S6). However, no *CaRLP*-DEG was identified between TMV-P2-inoculated and control plants, susceptible response (Supplementary Fig. S3). Heat map analysis divided the identified DEGs into four hierarchical clusters (Fig. 2a and 2b). In each cluster, *CaRLP*-DEGs identified between TMV-P0 vs. control treatments showed dynamic expression patterns, unlike those identified in TMV-P2 vs. control and PepMoV vs. control treatments. Cluster 1 was enriched in *CaRLPs* down-regulated in TMV-P0- and PepMoV-infected plants at 72 h post-inoculation (hpi). *CaRLP*-DEGs in clusters 2, 3, and 4 were up-regulation at later time points, mainly in TMV-P0-inoculated plants. These results indicate that several *CaRLPs* are involved in the response to viral pathogens.

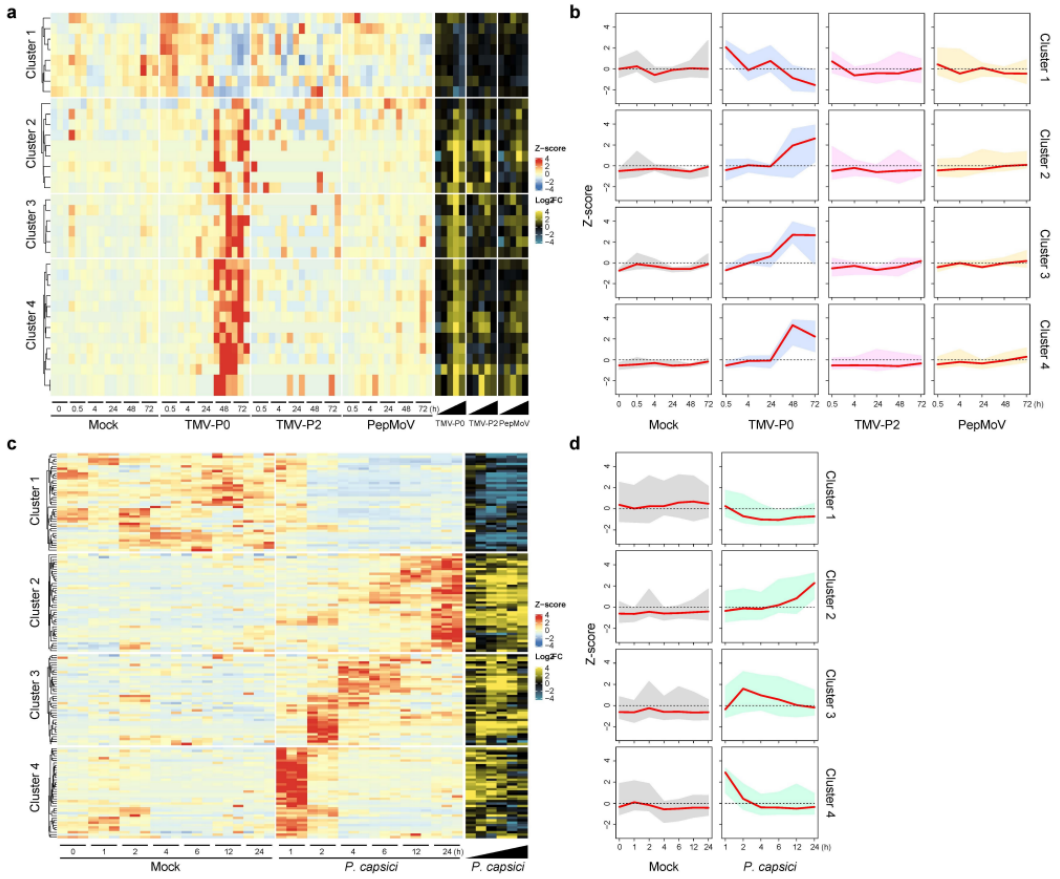

Fig. 2. Analysis of *CaRLP* expression patterns during pathogen infection. (a) Heat map displaying the time-course expression profiles of differentially expressed genes (DEGs) identified in plants treated with TMV-P0, TMV-P2, and PepMoV. The left hand side (red to blue scale) and right hand side (yellow to blue scale) of the heatmap indicate DEGs with z-score and $\log_2$(fold-change; FC) values, respectively. (b) Time-course analysis of the expression pattern of *CaRLP*-DEGs within clusters. Each cluster represents the hierarchical clustering numbers in the heatmap shown in (a). Numbers represent the mean z-score of DEGs, and red lines indicate median z-score within a cluster. (c) Heat map illustrating the time-course expression profiles of *CaRLP*-DEGs identified in plants treated with *P. capsici*. (d) Expression profiling of CaRLP-DEGs in clusters under *P. capsici* infection.

Next, we compared the transcriptome of *P. capsici*-inoculated plants at 1, 2, 4, 6, 12, and 24 hpi with that of control plants, and identified 158 *CaRLP*-DEGs (fold-change ≥ 2) at one or more time points (Fig. 2c, 2d, and Supplementary Table S7). This number was much higher than that obtained from virus-inoculated plants. These 158 *CaRLPs* were also divided into four clusters by hierarchical clustering analysis. *CaRLP*-DEGs overrepresented in clusters 1 and 4 were down-regulated, whereas those in cluster 2 were up-regulated at later time points. Genes in cluster 3 were highly expressed at 1 hpi, but their expression

decreased over time. A total of 31 *CaRLPs* were identified in both virus- and *P. capsici*-inoculated plants, and were referred to as common *CaRLP*-DEGs (Supplementary Table S6 and S7). Most of these 31 *CaRLP*-DEGs showed an increase in expression over time in both virus- and *P. capsici*-inoculated plants, and were classified into clusters 2, 3, and 4 in virus RNA-seq data and into clusters 2 and 3 in *P. capsici* RNA-seq data (Fig. 2). Taken together, comprehensive transcriptome profiling supported that CaRLPs are involved in an immune response against biotic stresses including viruses and oomycetes.

Construction of comprehensive co-expression networks of *CaRLPs* using RNA-seq data of pathogen-challenged pepper plants

To understand functional implications of *CaRLPs* expressed during pathogen infection, CaRLP-targeted GCNs were constructed using all 102 RNA-seq datasets (described above). Four GCNs involving CaRLPs as hub genes were identified, one each from the RNA-seq data of TMV-P0-, TMV-P2-, PepMoV-, and *P. capsici*-challenged plants; these CaRLP-GCNs consisted of 4,041 nodes with 11,825 edges, 1,073 nodes with 1,194 edges, 3,732 nodes with 7,933 edges and 10,878 nodes with 84,255 edges, respectively (Fig. 3a, 3b, 3c and 3d). Gene ontology (GO) enrichment analysis was performed for the modules in each of the GCNs identified. Various GO terms were enriched in the molecular function (MF), cellular component (CC) and biological process (BP) categories. Interestingly, two GO terms, “oxidation-reduction process” and “cellular oxidation detoxification,” were overrepresented in the BP category in the three pathogen treated datasets of ‘CM334,’ which showed resistance response to TMV-P0, PepMoV, and *P. capsici* (Fig. 3e). These two biological processes are known to be involved in plant immune response: reduction-oxidation changes occur in response to pathogen invasion and subsequently activate the plant immune function, i.e., HR, a programmed execution of challenged plant cells [47]; cellular oxidation detoxification has also been reported in plants under stress [48]. The GO term “phosphorylation” was enriched in the GCN from TMV-P2 treated RNA-seq dataset. Previously, [49] reported that phosphorylation is induced upon plant virus infection. These findings suggest that CaRLPs and the corresponding genes in GCNs are involved in biotic stress response in pepper. In addition, we carried out Kyoto Encyclopedia of Genes and Genomes (KEGG) pathway analysis of genes belonging to each GCN. The results showed enrichment of pathways associated with plant immune response such as “biosynthesis of antibiotics,” “phenylalanine metabolism” and “phenylpropanoid biosynthesis” in TMV-P0-, PepMoV-, and *P. capsici*-specific CaRLP-GCNs, respectively (Supplementary Fig. S4). Taken together, GO and KEGG enrichment analyses of GCNs showed that genes connected

234 with CaRLPs in GCNs are potentially involved in immune response in pepper.

235

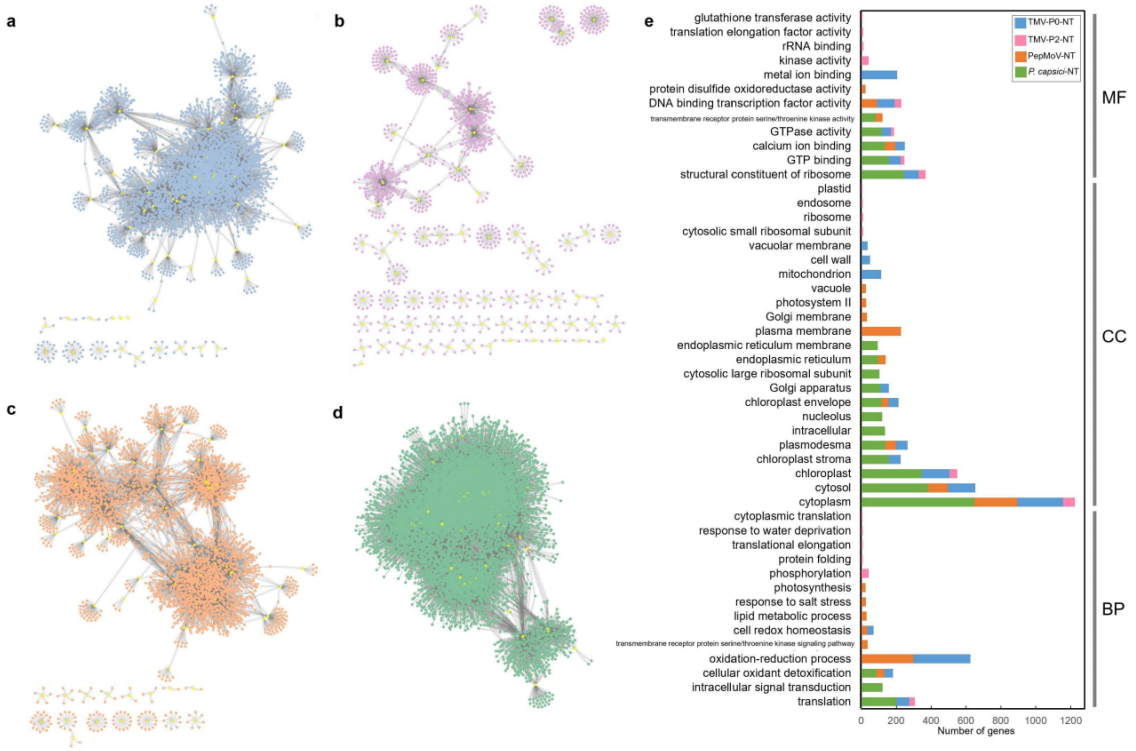

236

237 **Fig. 3. Analysis of the co-expression network (GCN) of *CaRLPs* identified using RNA-seq data**
238 **of biotic stress treated pepper plants.** (a–d) GCN comprising *CaRLP* hub genes identified in plants
239 treated with TMV-P0 (a), TMV-P2 (b), PepMoV (c) and *P. capsici* (d). Yellow dots in the GCN indicate
240 *CaRLPs*. (e) Top 20 GO terms significantly enriched in each of the four GCNs. The top 20 GO terms
241 ($P < 0.01$) were selected in order of the largest number of genes from each of the four GCNs. BP,
242 biological process; CC, cellular component; MF, molecular function.

243

244 **Identification of biotic stress-responsive core *CaRLPs***

245 To identify *CaRLPs* confer resistance to multiple pathogens, we merged the CaRLP-
246 GCNs derived from the RNA-seq datasets of TMV-P0-, PepMoV-, and *P. capsici*-infected
247 plants, thus constructing a universal resistance-responsive GCN (hereafter referred to as
248 RN). The RN contained eight modules (named as RN1–8), with a total 14 hub *CaRLPs* (Fig.
249 4a).

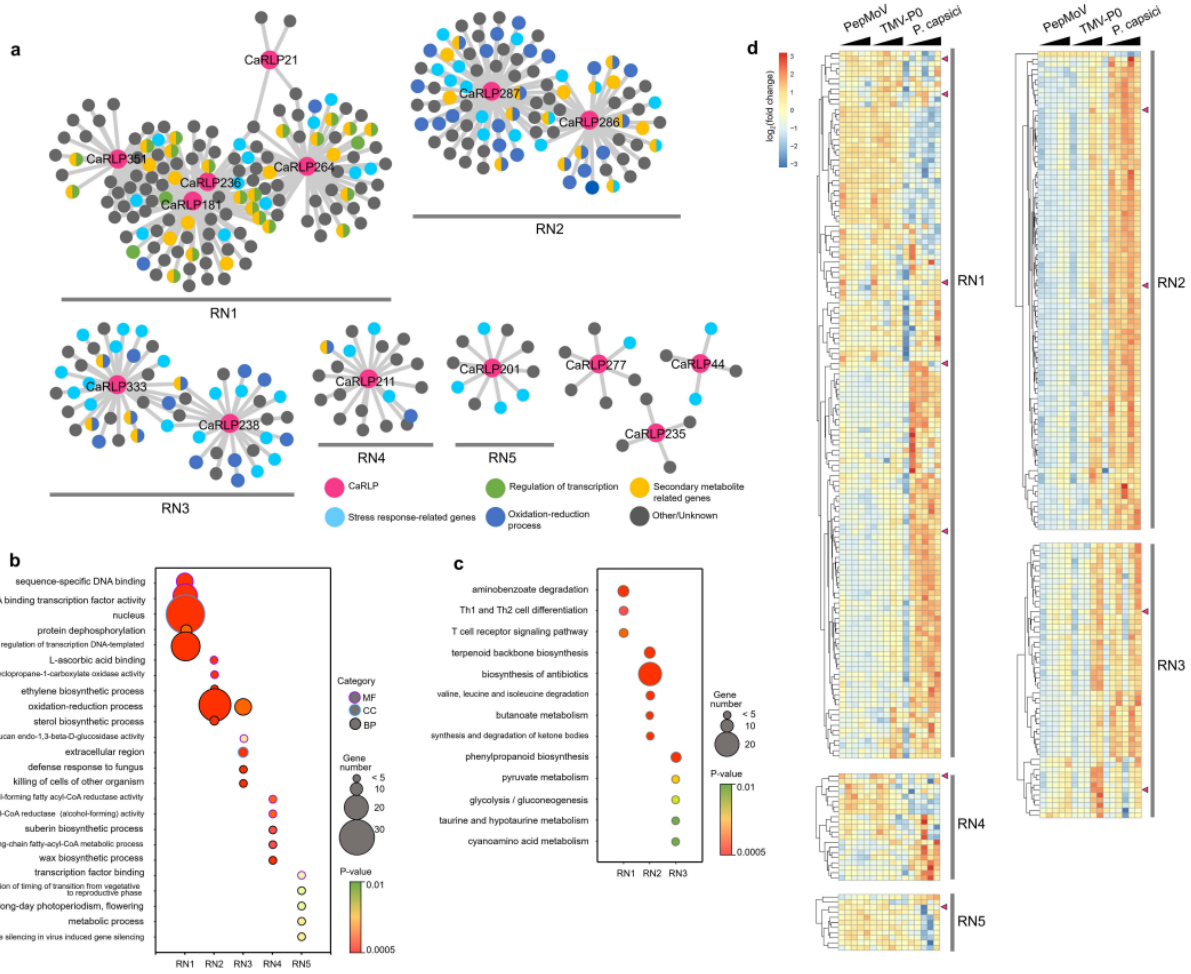

Fig. 4. Identification of biotic stress-responsive core *CaRLPs* in a universal GCN (a) Intersection of three GCNs of PepMoV-, TMV-P0- or *P. capsici*-infected plants. The co-expression network modules containing more than ten nodes were designated as RN1–RN5. Magenta nodes represent *CaRLPs*, and other colored nodes represent their annotated functions by GO analysis. (b) Top 5 GO categories enriched ($P < 0.01$) in five modules (RN1 to RN5). The Y-axis and X-axis in the bubble plot represent the GO category and different modules, respectively. The purple, blue, and black borders of the circle represent molecular function (MF), cellular component (CC), and biological process (BP), respectively. The size and color of each bubble represent the number of DEGs and *P*-value for each category, respectively. (c) Bubble plot showing the results of KEGG pathway enriched analysis of five co-expression modules (RN1 to RN5). The Y-axis and X-axis in the bubble plot represent the enriched KEGG pathways and network modules, respectively. The size and color of each bubble represent the number of DEGs and *P*-value for each category, respectively. (d) Expression profiles of genes in RN1–RN5 modules. Expression values were normalized relative to the value of control samples (Mock). Module names are indicated on the right hand side of the heatmap. Magenta triangles on the right side of the heat map indicate hub *CaRLPs* in each module. Black triangles on the top of the heat map represent the time-course of each pathogen infection.

Next, we performed GO and KEGG enrichment analyses and expression analysis to determine the biological processes and pathways affected during the plant immune responses of *CaRLPs* and associated pepper genes in RN. Thus, we focused on GO terms belonging to the BP category in these modules. Stress-related genes were enriched in RN modules (Fig. 4a and 4b). Notably, genes involved in stress response were higher enriched in RN2 and RN3 modules. We focused on GO terms belonging to the BP category in these modules. GO terms related plant defense mechanisms such as “oxidation-reduction process,” “sterol biosynthetic process” and “ethylene biosynthetic process” were highly enriched in the RN2 module, and “oxidation-reduction process,” “defense response to fungus,” and “cellular oxidant detoxification” were highly enriched in RN3. As mentioned above, oxidation-reduction and cellular oxidant detoxification occur in plants in response to pathogen attack. Most pathogenic fungi and oomycetes uptake sterols from the external environment, most likely from the host cell membrane, during pathogenesis[50]. In addition, ethylene acts as a signaling molecule during stress[51]. The results of KEGG pathway analysis revealed the enrichment of defense related pathways such as “biosynthesis of antibiotics,” “terpenoid backbone biosynthesis,” and “phenylpropanoid biosynthesis” in the RN (Fig. 4c). “Terpenoid backbone biosynthesis” and “phenylpropanoid biosynthesis” pathways produce secondary metabolites, which are involved in plant defense[52]. Taken together, these findings support that genes co-expressed with *CaRLPs* in the RN are involved in biotic stress response. We also examined the expression profiles of genes in the RN (Fig. 4d). Based on expression patterns, genes in RN1 were divided into two types: those highly up-regulated in response to both PepMoV and TMV-P0, and those up-regulated mainly in response to *P. capsici*. Genes in RN2 and RN3 modules were up-regulated in response to *P. capsici*. The expression of genes in each module was significantly correlated, indicating that these genes were tightly connected each other. Thus, these results suggest that hub *CaRLPs* in the RN play a role in resistance to multiple biotic stresses.

Functional validation of core *CaRLPs* involved in HR-like response to pathogen invasion

We hypothesized that core *CaRLPs*, i.e., hub genes in universal GCN, are involved in resistance response to biotic stresses. To decipher the core *CaRLPs* of the GCN, which potentially function in biotic stress response, we performed loss-of-function analysis of nine *CaRLP* genes; each of these genes was silenced by virus-induced gene silencing (VIGS) in the pepper cultivar ‘Nockwang.’ These nine genes included 2 genes not belonging to the RN (*CaRLP35* and *71*) and 7 core *CaRLPs* belonging to the RN (*CaRLP181*, *211*, *264*, *277*, *286*,

303 *287* and *351*); the remaining 7 of the 14 core *CaRLPs* were excluded from this analysis, as
304 their nucleotide sequence was none-specific for VIGS assay. VIGS constructs were
305 constructed by cloning a sequence unique to each of the nine *CaRLPs* into a *Tobacco rattle*
306 *virus* (TRV) vector; notably, because *CaRLP286* and *287* exhibit high level of sequence
307 similarity, both these genes could be silenced using a single construct containing a
308 sequence common to the two genes. The expression level of each *CaRLP* was significantly
309 lower in *CaRLP*-silenced pepper plants than in the *TRV2-GFP* control (Supplementary Fig.
310 S5), although no significant phenotypic difference was observed between *TRV2-CaRLP* and
311 control plants (Supplementary Fig. S6), indicating that the eight *CaRLP* constructs did not
312 affect the growth and development of pepper plants.

313 To investigate whether the silencing of *CaRLPs* affects HR, a form of programmed
314 cell death (PCD), upon TMV-P0 infection, we simultaneously inoculated *CaRLP*-silenced
315 pepper plants and control plants with TMV-P0, and monitored their phenotypes. The number
316 of HR lesions on TMV-P0-inoculated leaves was significantly lower in *TRV2-CaRLP264*, *-*
317 *277*, *-286/287* and *-351* lines than in *TRV2-GFP* plants at 48 hpi (Fig. 5a). The level of HR in
318 these four *CaRLP*-silenced lines was decreased by 0.22–0.72-fold compare with that in
319 control plants (Fig. 5b). By contrast, the silencing of other *CaRLP* genes did not cause any
320 significant change in the number of HR lesions. These results suggest that these *CaRLP*
321 genes are involved in the activation of defense mechanisms and PCD upon pathogen
322 infection in pepper.

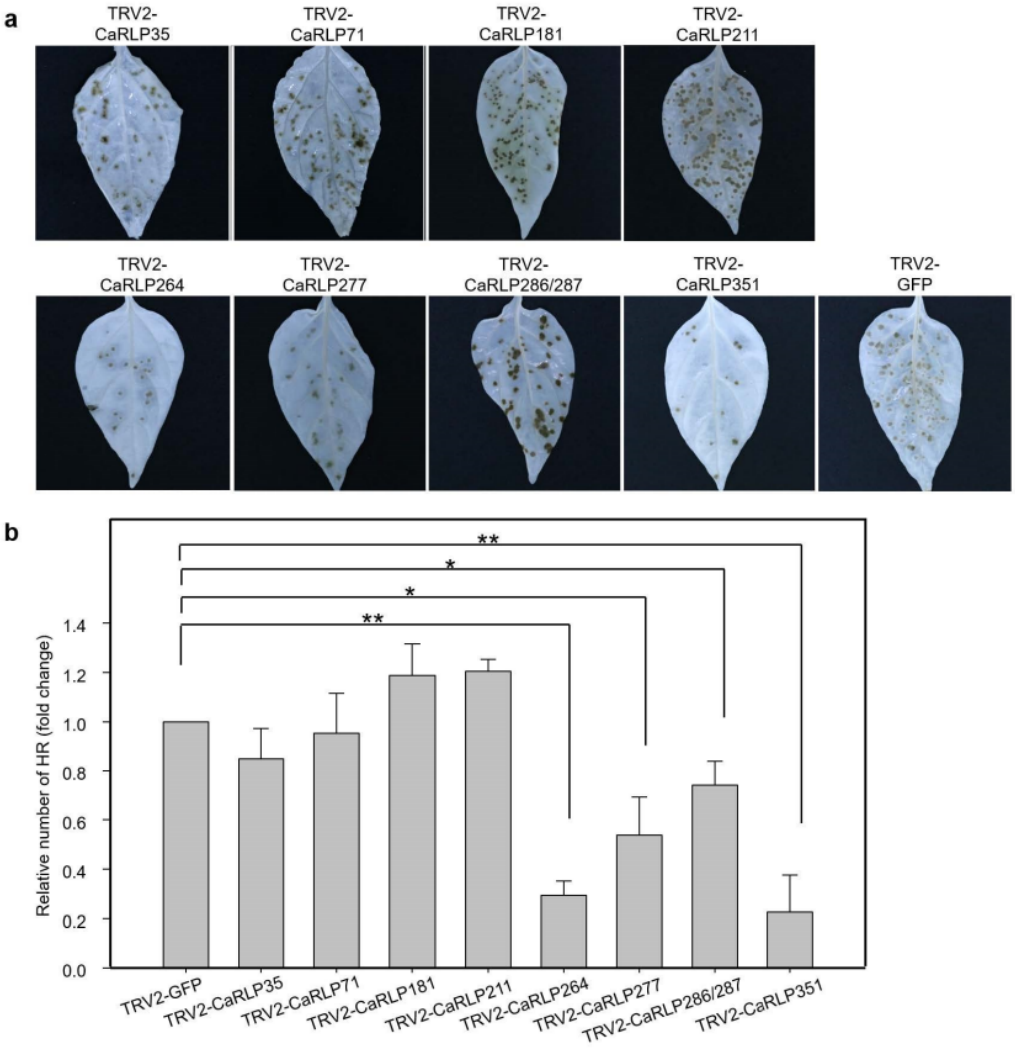

Fig. 5. Assessment of HR lesions in CaRLPs-silenced peppers to TMV-P0 infection. (a) Photographs showing TMV-P0-inoculated leaves of *CaRLP*-silenced plants. Photos were taken at 3 dpi. Chlorophyll was removed using ethyl alcohol. (b) Reduced HR lesion numbers in *CaRLP*-silenced plants inoculated with TMV-P0. Data indicate mean ± standard error (SE) of three independent experiments (n = 24). Asterisks indicate statistically significant differences compared with the *TRV2:GFP* control (*p < 0.05, **p < 0.01; Student's t-test).

Enhanced defense responses of core *CaRLP*-silenced pepper plants to various pathogens

To determine whether the core *CaRLPs* are involved in broad-spectrum resistance to various pathogens, we tested the response of *CaRLP*-silenced and *TRV2-GFP* control plants to *Xanthomonas axonopodis* pv. *glycines* 8ra (Xag8ra), *Ralstonia solanaceaerum* (Rsol) and *P. capsici*. We examined three different responses of *CaRLP*-silenced to the

above mentioned pathogens; for instance, non-host resistance to Xag8ra, host resistance to Rsol and susceptible response to *P. capsici*. We selected three *CaRLPs* (*CaRLP264*, *277* and *351*), which showed the most significant difference in the resistance response to TMV-P0 infection (Fig. 5).

To investigate the role of *CaRLPs* during HR response of non-host resistance[53,54], control plants (*TRV2-GFP*) and *CaRLP*-silenced plants (*TRV2-CaRLP264*, *-CaRLP277* and *-CaRLP351*) were infiltrated with Xag8ra (10^8 cfu/ml) (Fig. 6a). Xag8ra-inoculated plants of each *CaRLP*-silenced line showed significantly reduced HR-like cell death compared with control plants at 48 hpi. In addition, quantification of ion leakage from the inoculation-induced lesion showed that conductivity of each *CaRLP*-silenced line was approximately 1.5–2-fold lower than that of control plants (Fig. 6b). This suggests that the core *CaRLPs* play a crucial role in HR-based immunity of pepper plants against Xag8ra.

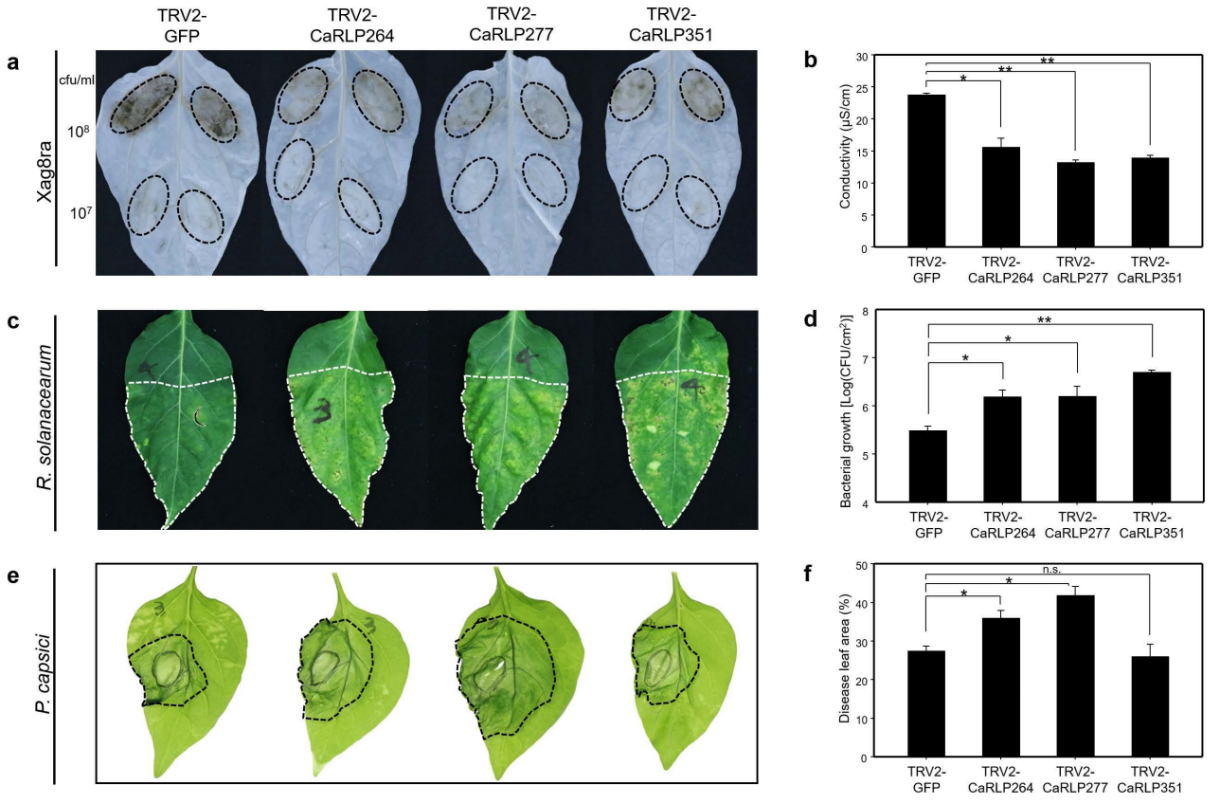

Fig. 6. Broad-spectrum resistance of core *CaRLP*-silenced peppers against various pathogens. (a) Response to Xag8ra inoculation on leaves of *CaRLP*-silenced plants. Photos were taken at 2 dpi. Chlorophyll was removed using ethyl alcohol. (b) Ion leakage data of Xag8ra-inoculated leaves. Ion leakage was measured using leaf disks from inoculation lesion of 10^8 cfu/ml of Xag8ra. (c) Response of *R. solanacearum* inoculation on leaves of *CaRLP*-silenced plants. Photos were taken at 8 dpi. (d) Bacterial growth of *R. solanacearum* in silenced plants. (e) Disease symptoms caused by *P. capsici* inoculation of the leaves of *CaRLP*-silenced plants and control plants. Photos were taken at 3 dpi. (f)

Disease lesion width normalized relative to the total leaf area. All data indicate mean ± SE from three independent experiments. Asterisks indicate statistically significant differences compared with the *TRV2:GFP* control (*p < 0.05, **p < 0.01; Student's *t*-test). n.s., not significant (p > 0.05).

Next, we performed leaf infiltration of Rsol, the causal agent of bacterial wilt disease, into *CaRLP*-silenced plants of *C. annuum* cultivar 'MC4,' which is resistant to Rsol[55]. Three *CaRLP*-silenced plants rapidly developed leaf wilting symptoms including necrosis and yellowing, as observed in susceptible plants but not in control plants (Fig. 6c). Furthermore, the growth of Rsol was increased significantly by approximately 5–15-fold in *CaRLP*-silenced plants compared with that in control plants at 5 dpi (Fig. 6d). These findings suggest that silencing *CaRLP264*, *CaRLP277*, and *CaRLP351* enhances the susceptibility to Rsol.

Finally, the leaves of CaRLP-silenced and control plants were also challenged with *P. capsici*, and disease development was examined at 3 dpi. The *CaRLP264*- and *CaRLP277*-silenced plants showed larger disease lesions than control plants, whereas *CaRLP351*-silenced plants showed no significant difference in lesion size compared with the control (Fig. 6e and 6f). This suggests that CaRLP263 and CaRLP277 are involved in the defense response to *P. capsici*. Taken together, plants of each *CaRLP*-silenced line consistently showed significant suppression of broad-spectrum defense against plant pathogens including viruses, bacteria, and oomycetes. Overall, our data suggest that core *CaRLPs* of the universal GCN perform conserved functions and confer resistance against multiple biotic stresses. Thus, these *CaRLPs* could be used to engineer cultivars with broad-spectrum resistance against diverse pathogens.

DISCUSSION

Plants sense pathogens via both cell surface and intracellular receptors. RLPs represent the primary layer of defense against pathogen infection in the innate immune system. In the present study, we identified a large number of *CaRLP* genes in the pepper genome, and selected variable biotic stress-responsive *CaRLP* genes as components of GCNs using 102 RNA-seq datasets. We demonstrated that three hub *CaRLPs* in the universal GCN confer broad-spectrum resistance against diverse pathogens.

A large percentage of genes in eukaryotic genomes are organized in clusters of various sizes and gene densities. Clusters containing resistance gene analogs (RGAs) including NLR, RLKs and RLPs have been reported in plants[24,44,56]. In tomato and pepper,

several genes related to RGAs are localized in clusters on various chromosomes[56-58]. Consistent with this data, we observed that *CaRLPs* belonging to the same phylogenetic group were mostly located in the same cluster, and thus showed uneven chromosomal distribution (Fig. 1). Information on the chromosomal location of *CaRLPs* would be highly valuable for the identification of functional RGAs.

GCNs could provide important clues for the characterization of novel genes, based on the analysis of potentially functionally associated co-expressed genes, using large-scale gene expression datasets[28]. Here, we attempted to infer the function of *CaRLPs* under various biotic stresses by the analysis of GCNs derived from a large number of RNA-seq datasets of *C. annuum* 'CM334.' GCNs were constructed using *CaRLPs* as hub genes in two steps: construction of large CaRLP-GCNs, based on the RNA-seq of each biotic stress, and construction of the intersection of CaRLP-GCNs, according to the type of biotic stress. Four large CaRLP-GCNs were constructed, each corresponding to four biotic stresses and containing 1,073–10,878 genes. These CaRLP-GCNs showed that *CaRLPs* are co-expressed with numerous other pepper genes under various biotic stresses. This result is consistent with previous studies, which showed that plant response to pathogens is extensively regulated at the transcriptional level[59-61].

The intersection of these four GCNs led to the construction of RN (Fig. 3 and Fig. 4). The RNA-seq data in this study was obtained from *C. annuum* cultivar 'CM334,' which is resistant to TMV-P0, PepMoV, and *P. capsici* but susceptible to TMV-P2. Consequently, GO enrichment analysis of genes in the RN revealed the enrichment of various stress related terms such as "oxidation-reduction process," "defense response to fungus," "response to biotic stimulus," and "cellular response to oxidative stress" (Fig. 4). In addition, numerous genes were enriched not only in stress related GO terms but also in transcription regulation (Fig. 4). Most of genes in the RN enriched under "regulation of transcription" encoded transcription factors, such as WRKY, AP2/ERF domain-containing proteins. These transcription factors play critical roles in abiotic and biotic stresses[62]. For example, WRKY proteins are involved in RLP-mediated defense response. Signal transduction of AtRLP51 was mediated by BDA1, an Ankyrin-repeat-containing protein with four transmembrane domains, to provoke plant defense response through the activation of WRKY70[63,64]. Taken together, these data suggest that *CaRLPs* in universal GCNs could be co-regulated with transcription factors under biotic stress.

We hypothesized that core *CaRLPs* in the universal GCN (RN) are involved in the response to biotic stresses. To test our hypothesis, we characterized the function of core *CaRLPs* using VIGS. We were not able to develop stable transgenic plants in pepper

because of the limitation of transgenic system for pepper and the low regeneration rate of pepper plants under in vitro conditions[65]. Of the six *CaRLPs* tested in this study, plants silenced for the expression of three *CaRLPs* showed reduced HR-like cell death upon TMV-P0 and Xag8ra inoculation (Fig. 5 and Fig. 6). By contrast, the silencing of each *CaRLP* significantly enhanced the disease susceptibility of pepper plants to *Rsol* and *P. capsici* compared with control plants (Fig. 6). These data suggest that the core *CaRLPs* in the universal GCN perform conserved functions and induce broad-spectrum resistance against plant pathogens. Thus, construction of a universal GCN from comprehensive transcriptome datasets could provide useful clues for uncovering the roles of genes in various biological processes.

Resistance gene-mediated immunity is highly effective immune systems against specific pathogens. On the other hands, PRRs, located on the plant cell surface, could confer resistance to a broad range of pathogens. In previous studies, few plant PRRs showed broad-spectrum resistance to pathogens. Expression of the Arabidopsis elongation factor Tu (EF-Tu), one of the PRRs, in *N. benthamiana* and tomato increased resistance to *Pseudomonas*, *Agrobacterium*, *Xanthomonas* and *Ralstonia*[4]. In potato, the elicitin response (ELR) receptor-like protein associates with the immune co-receptor BAK/SERK3, and mediates broad-spectrum recognition of elicitin proteins form several *Phytophthora* species[5]. In addition, suppression of the pepper lectin receptor kinase gene *CaLecRK-S.5*, which acts as a PRR, showed enhanced susceptibility to PepMoV, *Xanthomonas*, and*, P. capsici* [66]. In this study, through generation of a conserved GCN, we identified PRRs involved in broad-spectrum resistance against diverse plant pathogens. Three *CaRLPs* (*CaRLP264*, *277* and *351*) enhanced susceptibility to TMV-P0, *Xanthomonas*, *Ralstonia*, and *P. capsici* (Fig. 5 and Fig. 6). Thus, these *CaRLPs* could potentially be used to develop Solanaceae crop cultivars with broad-spectrum resistance against diverse pathogens. Overall, a universal GCN with comprehensive RNA-seq datasets could provide key insights to unveil gene functions in biological processes.

MATERIALS AND METHODS

Identification of *CaRLP* genes

A total of 13 characterized plant *RLP* genes (Supplementary Table S8) were used to obtain *CaRLP* gene sequences, which were used to build an hidden Markov model (HMM) domain with the HMMER software package (version 3.0; http://hmmer.org/), and identified

putative RLP-encoding genes against the *C. annuum* 'CM334' v. 1.55 genome. Then, tBLASTn searches were performed using the HMMER domain from amino acid sequences encoded by the pepper genome (threshold: 10^{-4}). Consequently, 600–750 hits to genes in the pepper genome were obtained from the BLAST output, accounting for 7,376 genes in total. This gene set was processed to remove redundant sequences by manual curation, thus obtaining 784 non-redundant candidate genes. The structure of CaRLPs was annotated using Pfam[67] and SMART [68] databases, and genes with kinase and NB-ARC domains were filtered out using Pfam IDs PF07714.12, PF00069.20 and PF00931, respectively. Finally, 438 CaRLPs from the 'CM334' genome.

Phylogenetic analysis and classification of CaRLPs

The CaRLPs were classified based on the results of phylogenetic analysis and sequence similarity-based clustering, as described previously[24,44]. Clustering analysis of full-length amino acid sequences of Arabidopsis, tomato, pepper and reported RLPs was performed by OrthoMCL[69]. RLPs within the same cluster were determined to be identical subgroups to the phylogenetic subgroups. RLPs clustered as singletons (mostly partial and short sequences) were identified using a BLASTP search against identified RLPs, and subgroups were assigned. We designated the known RLP names according to the corresponding pepper RLP groups.

A conserved domain of an HMM profile was built based on the amino acid sequence of conserved C3-D region[25] of known RLPs. A phylogenetic tree was constructed based on the C3-D domain of 56 AtRLPs[22,25], 176 SlRLPs[24], 438 CaRLPs, and 13 RLPs reported by HMM search (E-value < 0.001). *RLP* genes containing less than 80% of the full-length C3-D domain sequence were excluded. Multiple sequence alignment of the C3-D domains of RLPs was performed using MUSCLE (http://www.ebi.ac.uk/Tools/msa/muscle/). The alignment result was used to build a phylogenetic tree using PhyML (http://www.phylogeny.fr/), with default parameters (SH-like approximate likelihood-ratio test for branch support), and the resulting phylogenetic trees were edited using the MEGA8 software (http://www.megasoftware.net/).

Chromosomal location, physical cluster, and motif analyses

The chromosomal location of *CaRLPs* was determined based on the genome sequence of the pepper cultivar 'CM334'[42]. MapChart[70] was used to draw the location of RLPs on chromosomes. Physical clustering of *CaRLPs* in the pepper genome was determined based on two criteria: 1) the gene cluster spans a region of 200 kb or less; and 2)

494 the cluster contains less than eight non-*RLP* genes between two *CaRLPs*[24,44].

495 Conserved motifs in CaRLPs were identified using the MEME suite (http://meme-
496 suite.org/tools/meme), with default settings except for the following parameters: maximum
497 number of motifs, 20; minimum width of motifs, 15; maximum width of motifs, 200.
498 Subsequently, MAST (http://meme-suite.org/tools/mast) was carried out on datasets
499 including protein sequences of CaRLPs and known RLPs with default E-values.

500

501 **RNA-seq library construction**

502 Changes in the expression profiles of *CaRLPs* upon *P. capsici* infection were
503 investigated in the pepper cultivar 'CM334' by RNA-seq analysis. Leaves of 4–5-week-old
504 pepper plants were infiltrated with *P. capsici* (5×10^4 zoospore/ml), and infected leaves were
505 collected at 0, 1, 2, 4, 6, 12, and 24 hpi in three biological replicates. Total RNA was isolated
506 using the TRIzol Reagent (Invitrogen, Carlsbad, CA, USA), according to the manufacturer's
507 instructions. RNA-seq libraries were constructed as described previously[45]. All 39 RNA-seq
508 libraries (21 libraries of *P. capsici*-infected samples, and 18 libraries of control samples) were
509 sequenced using Illumina HiSeq 2000 (Illumina Inc., San Diego, CA, USA).

510

511 **RNA-seq data analysis**

512 Quality control of RNA-seq data of *P. capsici*-infected samples was performed by
513 removing low-quality reads and possible contaminants, as described previously[40,41]. Adapter
514 and low-quality sequences were filtered using Cutadapt[71] and Trimmomatic[72], based on the
515 Phred quality threshold of 20. In addition, transcriptome data of pepper plants infected by
516 TMV-P0, TMV-P2, and PepMoV were obtained from previous studies[43,45] to analyze the
517 expression of *CaRLPs*.

518

519 **Gene expression analysis**

520 The expression profiles of *CaRLPs* under biotic stresses were analyzed using RNA-
521 seq data of TMV-P0-, TMV-P2- and PepMoV-inoculated pepper plants and that of *P. capsici*-
522 inoculated pepper plants. Sequence reads from all RNA-seq datasets were aligned to the
523 'CM334' reference genome using Hisat2[73]. Filtered clean reads of virus RNA-seq and *P.*
524 *capsici* RNA-seq were normalized into reads per kilobase per million mapped reads and
525 fragments per kilobase per million mapped fragments, respectively. DEGs were identified

using the DESeq2 package (FDR < 0.05)[74]. The expression patterns of DEGs were visualized using ComplexHeatmap[75].

GCN construction and GO and KEGG enrichment analyses

The GCN was constructed from 102 RNA-seq datasets using the exp2net function of the mlDNA package[76], and inferred using the Pearson's product moment correlation coefficient at a significance level of $P < 0.01$. In next step, genes co-expressed with *CaRLPs* were identified by filtering the correlation coefficient ($|r| > 0.8$) and only directed interaction. The GCN was visualized using Cytoscape v3.4.0[77]. To identify gene networks involved in different stress responses, GCNs containing *CaRLP* genes were extracted by different combinations of all stresses using Merge Tools in Cytoscpae. GO and KEGG enrichment analyses were performed by GOseq[78] in R packages using Pepper v1.55 genome annotation from BLAST2GO[79].

VIGS

Pepper cultivars *C. annuum* 'Nockwang' and 'MC4' were used to analyze the effect of *CaRLP* gene silencing on defense response. Seedlings with two fully expanded cotyledons were for the VIGS assay. The 3' or 5' untranslated region (UTR) of eight *CaRLP* genes (*CaRLP35*, *CaRLP71*, *CaRLP181*, *CaRLP211*, *CaRLP264*, *CaRLP277*, *CaRLP286*/*287* and *CaRLP351*) was amplified and cloned into the pTRV2 vector. The resulting pTRV2-CaRLP constructs were transformed into *Agrobacterium tumefaciens* strain GV3101. VIGS was conducted as described previously[80]. Plants infiltrated with *pTRV2-GFP* or *pTRV2-PDS* with pTRV1 were used as a control. One leaf was harvested from each *CaRLP*-silenced plant for RNA extraction and the measurement of silencing efficiency.

Pathogen inoculation

All pathogen inoculations were performed on the 3rd and 4th true leaves of *CaRLP*-silenced and control pepper plants at 4–5 weeks after the VIGS assay. Plants were challenged with three different types of pathogens (including viruses (TMV-P0, Xag8ra), bacteria (Rsol) and oomycete (*P. capsici*). The TMV-P0 inoculum was prepared from 1 g of infected *N. benthamiana* leaves using 10 ml of 0.1 M phosphate buffer (pH 7.0). TMV-inoculated leaves were monitored and harvested at 3 days post-inoculation (dpi). To assess the formation of lesions on TMV-inoculated leaves, chlorophyll was removed using ethyl

559 alcohol. To conduct the Rsol-response assay, Rsol 'SL1931' was cultured first in TZC agar
560 medium at 28°C for 2 days and then in CPG medium at 28°C for 24 h, and then suspended
561 in distilled sterile water. The Rsol suspension was diluted to a concentration of 10^5 cfu/ml,
562 and infiltrated into the leaves of *CaRLP*-silenced pepper plants. Subsequently, Rsol-
563 inoculated plants were grown in a growth chamber at 28 ± 2°C, 70% relative humidity and
564 16h-light/8h-dark photoperiod, and inoculated leaves were harvested at 5 dpi. Inocula of
565 Xag8ra and *P. capsici* were prepared as described previously [53,80]. The Xag8ra culture was
566 suspended in 10 mM $MgCl_2$, and then diluted to 10^7 and 10^8 cfu/ml concentrations. The
567 Xag8ra-inoculated leaves were harvested at 2 dpi and used for measuring conductivity and
568 detecting cell death. To prepare the *P. capsici* inoculum, the released zoospores were
569 collected and diluted in distilled sterile water to a concentration of 1×10^5 spores/ml. The *P.*
570 *capsici* suspension was infiltrated into the leaves of *CaRLP*-silenced pepper plants, and
571 harvested at 3 dpi. All pathogen inoculation were conducted in at least three independent
572 experiments, with 8–12 plants for per experiment.

573

574 **Quantification of ion leakage**

575 Ion leakage from Xag8ra-inoculated leaves was measured as described previously[53].
576 Sixteen leaf disks (each 1 cm in diameter) were excised from 4–6 plants of each *CaRLP*-
577 silenced line, and floated on 15 ml of sterile distilled water for 2 h at room temperature. Then,
578 the electrolyte leakage from leaf discs was measured by a conductivity meter (Eutech con
579 510; Thermo scientific, Waltham, MA, USA).

580

581 **Bacterial cell counting**

582 In Rsol-inoculated pepper plants, bacterial cell growth was measured in planta, as
583 described previously[55], with slight modifications. Six leaf disks (each 1 cm in diameter) were
584 excised from Rsol-inoculated leaves of 3–4 plants of each *CaRLP*-silenced line at 5dpi. Leaf
585 disks were ground in sterile distilled water, and serial dilutions were plated on CPG agar
586 medium supplemented with gentamycin. The plates were incubated at 28°C, and bacterial
587 cells were counted after 2 days.

588

589 **ACKNOWLEDGEMENTS**

590 This research was supported by the National Research Foundation of Korea (NRF) funded
591 by the Korean Government (NRF-2017R1E1A1A01072843 and 2019R1C1C1007472). We

appreciate the support from the KRIBB initiative program.

CONFLICT OF INTERESTS

The authors have declared that no competing interests exist.

AUTHOR CONTRIBUTIONS

WHK, BP, and JSK collected samples and performed experiments. YMK and JL generated RNA-seq data. NK and WHK analyzed transcriptome. WHK and SIY conceived and designed the experiments, organized and wrote the manuscript, and supervised the project. All authors read and approved the final manuscript.

603 **References**

604

605 1 Lee, H. A. & Yeom, S. I. Plant NB-LRR proteins: tightly regulated sensors in a complex
606 manner. *Brief Funct Genomics* **14**, 233-242, doi:10.1093/bfgp/elv012 (2015).
607 2 Wan, W. L., Frohlich, K., Pruitt, R. N., Nurnberger, T. & Zhang, L. Plant cell surface immune
608 receptor complex signaling. *Curr Opin Plant Biol* **50**, 18-28, doi:10.1016/j.pbi.2019.02.001
609 (2019).
610 3 Albert, I., Hua, C., Nurnberger, T., Pruitt, R. N. & Zhang, L. Surface Sensor Systems in Plant
611 Immunity. *Plant Physiol* **182**, 1582-1596, doi:10.1104/pp.19.01299 (2020).
612 4 Lacombe, S. *et al.* Interfamily transfer of a plant pattern-recognition receptor confers broad-
613 spectrum bacterial resistance. *Nat Biotechnol* **28**, 365-369, doi:10.1038/nbt.1613 (2010).
614 5 Du, J. *et al.* Elicitin recognition confers enhanced resistance to Phytophthora infestans in
615 potato. *Nat Plants* **1**, 15034, doi:10.1038/nplants.2015.34 (2015).
616 6 Dixon, M. S., Hatzixanthis, K., Jones, D. A., Harrison, K. & Jones, J. D. The tomato Cf-5
617 disease resistance gene and six homologs show pronounced allelic variation in leucine-rich
618 repeat copy number. *Plant Cell* **10**, 1915-1925, doi:10.1105/tpc.10.11.1915 (1998).
619 7 Dixon, M. S. *et al.* The tomato Cf-2 disease resistance locus comprises two functional genes
620 encoding leucine-rich repeat proteins. *Cell* **84**, 451-459, doi:10.1016/s0092-8674(00)81290-8
621 (1996).
622 8 Takken, F. L., Schipper, D., Nijkamp, H. J. & Hille, J. Identification and Ds-tagged isolation of a
623 new gene at the Cf-4 locus of tomato involved in disease resistance to Cladosporium fulvum
624 race 5. *Plant J* **14**, 401-411, doi:10.1046/j.1365-313x.1998.00135.x (1998).
625 9 Thomas, C. M. *et al.* Characterization of the tomato Cf-4 gene for resistance to Cladosporium
626 fulvum identifies sequences that determine recognitional specificity in Cf-4 and Cf-9. *Plant*
627 *Cell* **9**, 2209-2224, doi:10.1105/tpc.9.12.2209 (1997).
628 10 Hegenauer, V. *et al.* Detection of the plant parasite Cuscuta reflexa by a tomato cell surface
629 receptor. *Science* **353**, 478-481, doi:10.1126/science.aaf3919 (2016).
630 11 Jehle, A. K. *et al.* The receptor-like protein ReMAX of Arabidopsis detects the microbe-
631 associated molecular pattern eMax from Xanthomonas. *Plant Cell* **25**, 2330-2340,
632 doi:10.1105/tpc.113.110833 (2013).
633 12 Kawchuk, L. M. *et al.* Tomato Ve disease resistance genes encode cell surface-like receptors.
634 *Proc Natl Acad Sci U S A* **98**, 6511-6515, doi:10.1073/pnas.091114198 (2001).
635 13 Larkan, N. J. *et al.* The Brassica napus blackleg resistance gene LepR3 encodes a receptor-
636 like protein triggered by the Leptosphaeria maculans effector AVRLM1. *New Phytol* **197**, 595-
637 605, doi:10.1111/nph.12043 (2013).
638 14 Ron, M. & Avni, A. The receptor for the fungal elicitor ethylene-inducing xylanase is a member
639 of a resistance-like gene family in tomato. *Plant Cell* **16**, 1604-1615, doi:10.1105/tpc.022475
640 (2004).
641 15 Shen, Y. & Diener, A. C. Arabidopsis thaliana resistance to fusarium oxysporum 2 implicates

642 tyrosine-sulfated peptide signaling in susceptibility and resistance to root infection. *PLoS*
643 *Genet* **9**, e1003525, doi:10.1371/journal.pgen.1003525 (2013).
644 16 Steinbrenner, A. D. *et al.* A receptor-like protein mediates plant immune responses to
645 herbivore-associated molecular patterns. *Proc Natl Acad Sci U S A* **117**, 31510-31518,
646 doi:10.1073/pnas.2018415117 (2020).
647 17 Vinatzer, B. A. *et al.* Apple contains receptor-like genes homologous to the Cladosporium
648 fulvum resistance gene family of tomato with a cluster of genes cosegregating with Vf apple
649 scab resistance. *Mol Plant Microbe Interact* **14**, 508-515, doi:10.1094/MPMI.2001.14.4.508
650 (2001).
651 18 Zhang, B. *et al.* BrRLP48, Encoding a Receptor-Like Protein, Involved in Downy Mildew
652 Resistance in Brassica rapa. *Front Plant Sci* **9**, 1708, doi:10.3389/fpls.2018.01708 (2018).
653 19 Jeong, S., Trotochaud, A. E. & Clark, S. E. The Arabidopsis CLAVATA2 gene encodes a
654 receptor-like protein required for the stability of the CLAVATA1 receptor-like kinase. *Plant Cell*
655 **11**, 1925-1934, doi:10.1105/tpc.11.10.1925 (1999).
656 20 Nadeau, J. A. & Sack, F. D. Control of stomatal distribution on the Arabidopsis leaf surface.
657 *Science* **296**, 1697-1700, doi:10.1126/science.1069596 (2002).
658 21 Taguchi-Shiobara, F., Yuan, Z., Hake, S. & Jackson, D. The fasciated ear2 gene encodes a
659 leucine-rich repeat receptor-like protein that regulates shoot meristem proliferation in maize.
660 *Genes Dev* **15**, 2755-2766, doi:10.1101/gad.208501 (2001).
661 22 Wang, G. *et al.* A genome-wide functional investigation into the roles of receptor-like proteins
662 in Arabidopsis. *Plant Physiol* **147**, 503-517, doi:10.1104/pp.108.119487 (2008).
663 23 Petre, B., Hacquard, S., Duplessis, S. & Rouhier, N. Genome analysis of poplar LRR-RLP
664 gene clusters reveals RISP, a defense-related gene coding a candidate endogenous peptide
665 elicitor. *Front Plant Sci* **5**, 111, doi:10.3389/fpls.2014.00111 (2014).
666 24 Kang, W. H. & Yeom, S. I. Genome-wide Identification, Classification, and Expression
667 Analysis of the Receptor-Like Protein Family in Tomato. *Plant Pathol J* **34**, 435-444,
668 doi:10.5423/PPJ.OA.02.2018.0032 (2018).
669 25 Fritz-Laylin, L. K., Krishnamurthy, N., Tor, M., Sjolander, K. V. & Jones, J. D. Phylogenomic
670 analysis of the receptor-like proteins of rice and Arabidopsis. *Plant Physiol* **138**, 611-623,
671 doi:10.1104/pp.104.054452 (2005).
672 26 Yang, H., Bayer, P. E., Tirnaz, S., Edwards, D. & Batley, J. Genome-Wide Identification and
673 Evolution of Receptor-Like Kinases (RLKs) and Receptor like Proteins (RLPs) in Brassica
674 juncea. *Biology (Basel)* **10**, doi:10.3390/biology10010017 (2020).
675 27 Restrepo-Montoya, D., Brueggeman, R., McClean, P. E. & Osorno, J. M. Computational
676 identification of receptor-like kinases "RLK" and receptor-like proteins "RLP" in legumes. *BMC*
677 *Genomics* **21**, 459, doi:10.1186/s12864-020-06844-z (2020).
678 28 Li, Y., Pearl, S. A. & Jackson, S. A. Gene Networks in Plant Biology: Approaches in
679 Reconstruction and Analysis. *Trends Plant Sci* **20**, 664-675, doi:10.1016/j.tplants.2015.06.013
680 (2015).
681 29 Sun, B. M. *et al.* Coexpression network analysis reveals an MYB transcriptional activator

682 involved in capsaicinoid biosynthesis in hot peppers. *Hortic Res-England* **7**, doi:ARTN 162
683 10.1038/s41438-020-00381-2 (2020).
684 30 Zheng, J. *et al.* Co-expression analysis aids in the identification of genes in the cuticular wax
685 pathway in maize. *Plant Journal* **97**, 530-542, doi:10.1111/tpj.14140 (2019).
686 31 Ruprecht, C., Vaid, N., Proost, S., Persson, S. & Mutwil, M. Beyond Genomics: Studying
687 Evolution with Gene Coexpression Networks. *Trends Plant Sci* **22**, 298-307,
688 doi:10.1016/j.tplants.2016.12.011 (2017).
689 32 Amrine, K. C., Blanco-Ulate, B. & Cantu, D. Discovery of core biotic stress responsive genes
690 in Arabidopsis by weighted gene co-expression network analysis. *PLoS One* **10**, e0118731,
691 doi:10.1371/journal.pone.0118731 (2015).
692 33 Dossa, K. *et al.* Depicting the Core Transcriptome Modulating Multiple Abiotic Stresses
693 Responses in Sesame (Sesamum indicum L.). *Int J Mol Sci* **20**, doi:10.3390/ijms20163930
694 (2019).
695 34 Zhu, M. *et al.* WGCNA Analysis of Salt-Responsive Core Transcriptome Identifies Novel Hub
696 Genes in Rice. *Genes (Basel)* **10**, doi:10.3390/genes10090719 (2019).
697 35 Ruprecht, C. *et al.* FamNet: A Framework to Identify Multiplied Modules Driving Pathway
698 Expansion in Plants. *Plant Physiol* **170**, 1878-1894, doi:10.1104/pp.15.01281 (2016).
699 36 Ichihashi, Y. *et al.* Evolutionary developmental transcriptomics reveals a gene network module
700 regulating interspecific diversity in plant leaf shape. *Proc Natl Acad Sci U S A* **111**, E2616-
701 2621, doi:10.1073/pnas.1402835111 (2014).
702 37 Chang, Y. M. *et al.* Comparative transcriptomics method to infer gene coexpression networks
703 and its applications to maize and rice leaf transcriptomes. *Proc Natl Acad Sci U S A* **116**,
704 3091-3099, doi:10.1073/pnas.1817621116 (2019).
705 38 Gerstein, M. B. *et al.* Comparative analysis of the transcriptome across distant species.
706 *Nature* **512**, 445-448, doi:10.1038/nature13424 (2014).
707 39 Mutwil, M. *et al.* PlaNet: combined sequence and expression comparisons across plant
708 networks derived from seven species. *Plant Cell* **23**, 895-910, doi:10.1105/tpc.111.083667
709 (2011).
710 40 Kang, W. H. *et al.* Transcriptome profiling of abiotic responses to heat, cold, salt, and osmotic
711 stress of Capsicum annuum L. *Sci Data* **7**, 17, doi:10.1038/s41597-020-0352-7 (2020).
712 41 Lee, J. *et al.* Comprehensive transcriptome resource for response to phytohormone-induced
713 signaling in Capsicum annuum L. *BMC Res Notes* **13**, 440, doi:10.1186/s13104-020-05281-1
714 (2020).
715 42 Kim, S. *et al.* New reference genome sequences of hot pepper reveal the massive evolution
716 of plant disease-resistance genes by retroduplication. *Genome Biol* **18**, 210,
717 doi:10.1186/s13059-017-1341-9 (2017).
718 43 Kim, M. S. *et al.* Global gene expression profiling for fruit organs and pathogen infections in
719 the pepper, Capsicum annuum L. *Sci Data* **5**, 180103, doi:10.1038/sdata.2018.103 (2018).
720 44 Seo, E., Kim, S., Yeom, S. I. & Choi, D. Genome-Wide Comparative Analyses Reveal the
721 Dynamic Evolution of Nucleotide-Binding Leucine-Rich Repeat Gene Family among

Solanaceae Plants. *Front Plant Sci* **7**, 1205, doi:10.3389/fpls.2016.01205 (2016).

45 Kang, W. H., Kim, S., Lee, H. A., Choi, D. & Yeom, S. I. Genome-wide analysis of Dof transcription factors reveals functional characteristics during development and response to biotic stresses in pepper. *Sci Rep* **6**, 33332, doi:10.1038/srep33332 (2016).

46 Kim, N., Kang, W. H., Lee, J. & Yeom, S. I. Development of Clustered Resistance Gene Analogs-Based Markers of Resistance to Phytophthora capsici in Chili Pepper. *Biomed Res Int* **2019**, 1093186, doi:10.1155/2019/1093186 (2019).

47 Frederickson Matika, D. E. & Loake, G. J. Redox regulation in plant immune function. *Antioxid Redox Signal* **21**, 1373-1388, doi:10.1089/ars.2013.5679 (2014).

48 Mittler, R. Oxidative stress, antioxidants and stress tolerance. *Trends Plant Sci* **7**, 405-410, doi:10.1016/s1360-1385(02)02312-9 (2002).

49 Wu, L. *et al.* Phosphoproteomic analysis of the resistant and susceptible genotypes of maize infected with sugarcane mosaic virus. *Amino Acids* **47**, 483-496, doi:10.1007/s00726-014-1880-2 (2015).

50 Kazan, K. & Gardiner, D. M. Targeting pathogen sterols: Defence and counterdefence? *PLoS Pathog* **13**, e1006297, doi:10.1371/journal.ppat.1006297 (2017).

51 van Loon, L. C., Geraats, B. P. & Linthorst, H. J. Ethylene as a modulator of disease resistance in plants. *Trends Plant Sci* **11**, 184-191, doi:10.1016/j.tplants.2006.02.005 (2006).

52 Erb, M. & Kliebenstein, D. J. Plant Secondary Metabolites as Defenses, Regulators, and Primary Metabolites: The Blurred Functional Trichotomy. *Plant Physiol* **184**, 39-52, doi:10.1104/pp.20.00433 (2020).

53 Yeom, S. I. *et al.* Use of a secretion trap screen in pepper following Phytophthora capsici infection reveals novel functions of secreted plant proteins in modulating cell death. *Mol Plant Microbe Interact* **24**, 671-684, doi:10.1094/MPMI-08-10-0183 (2011).

54 Yi, S. Y. *et al.* A novel pepper (Capsicum annuum) receptor-like kinase functions as a negative regulator of plant cell death via accumulation of superoxide anions. *New Phytol* **185**, 701-715, doi:10.1111/j.1469-8137.2009.03095.x (2010).

55 Kwon, J.-S., Nam, J.-Y., Yeom, S.-I. & Kang, W.-H. Leaf-to-whole plant spread bioassay for pepper and *Ralstonia solanacearum* interaction determines inheritance of resistance to bacterial wilt for further breeding. *bioRxiv*, 2021.2001.2027.428365, doi:10.1101/2021.01.27.428365 (2021).

56 Andolfo, G. *et al.* Overview of tomato (Solanum lycopersicum) candidate pathogen recognition genes reveals important Solanum R locus dynamics. *New Phytol* **197**, 223-237, doi:10.1111/j.1469-8137.2012.04380.x (2013).

57 Kim, S. B. *et al.* Divergent evolution of multiple virus-resistance genes from a progenitor in Capsicum spp. *New Phytol* **213**, 886-899, doi:10.1111/nph.14177 (2017).

58 Kruijt, M., MJ, D. E. K. & de Wit, P. J. Receptor-like proteins involved in plant disease resistance. *Mol Plant Pathol* **6**, 85-97, doi:10.1111/j.1364-3703.2004.00264.x (2005).

59 Buscaill, P. & Rivas, S. Transcriptional control of plant defence responses. *Curr Opin Plant Biol* **20**, 35-46, doi:10.1016/j.pbi.2014.04.004 (2014).

762 60 Eulgem, T. Regulation of the Arabidopsis defense transcriptome. *Trends Plant Sci* **10**, 71-78,
763 doi:10.1016/j.tplants.2004.12.006 (2005).
764 61 Tsuda, K. & Somssich, I. E. Transcriptional networks in plant immunity. *New Phytol* **206**, 932-
765 947, doi:10.1111/nph.13286 (2015).
766 62 Javed, T. *et al.* Transcription Factors in Plant Stress Responses: Challenges and Potential for
767 Sugarcane Improvement. *Plants (Basel)* **9**, doi:10.3390/plants9040491 (2020).
768 63 Yang, Y. *et al.* The ankyrin-repeat transmembrane protein BDA1 functions downstream of the
769 receptor-like protein SNC2 to regulate plant immunity. *Plant Physiol* **159**, 1857-1865,
770 doi:10.1104/pp.112.197152 (2012).
771 64 Zhang, Y. *et al.* Arabidopsis snc2-1D activates receptor-like protein-mediated immunity
772 transduced through WRKY70. *Plant Cell* **22**, 3153-3163, doi:10.1105/tpc.110.074120 (2010).
773 65 Kothari, S. L., Joshi, A., Kachhwaha, S. & Ochoa-Alejo, N. Chilli peppers--a review on tissue
774 culture and transgenesis. *Biotechnol Adv* **28**, 35-48, doi:10.1016/j.biotechadv.2009.08.005
775 (2010).
776 66 Woo, J. Y., Jeong, K. J., Kim, Y. J. & Paek, K. H. CaLecRK-S.5, a pepper L-type lectin
777 receptor kinase gene, confers broad-spectrum resistance by activating priming. *J Exp Bot* **67**,
778 5725-5741, doi:10.1093/jxb/erw336 (2016).
779 67 Finn, R. D. *et al.* Pfam: the protein families database. *Nucleic Acids Res* **42**, D222-230,
780 doi:10.1093/nar/gkt1223 (2014).
781 68 Schultz, J., Milpetz, F., Bork, P. & Ponting, C. P. SMART, a simple modular architecture
782 research tool: identification of signaling domains. *Proc Natl Acad Sci U S A* **95**, 5857-5864,
783 doi:10.1073/pnas.95.11.5857 (1998).
784 69 Li, L., Stoeckert, C. J., Jr. & Roos, D. S. OrthoMCL: identification of ortholog groups for
785 eukaryotic genomes. *Genome Res* **13**, 2178-2189, doi:10.1101/gr.1224503 (2003).
786 70 Voorrips, R. E. MapChart: software for the graphical presentation of linkage maps and QTLs.
787 *J Hered* **93**, 77-78, doi:10.1093/jhered/93.1.77 (2002).
788 71 Martin, M. Cutadapt removes adapter sequences from high-throughput sequencing reads.
789 *EMBnet.journal* **17**, doi:https://doi.org/10.14806/ej.17.1.200 (2011).
790 72 Bolger, A. M., Lohse, M. & Usadel, B. Trimmomatic: a flexible trimmer for Illumina sequence
791 data. *Bioinformatics* **30**, 2114-2120, doi:10.1093/bioinformatics/btu170 (2014).
792 73 Kim, D., Langmead, B. & Salzberg, S. L. HISAT: a fast spliced aligner with low memory
793 requirements. *Nat Methods* **12**, 357-360, doi:10.1038/nmeth.3317 (2015).
794 74 Love, M. I., Huber, W. & Anders, S. Moderated estimation of fold change and dispersion for
795 RNA-seq data with DESeq2. *Genome Biol* **15**, 550, doi:10.1186/s13059-014-0550-8 (2014).
796 75 Gu, Z., Eils, R. & Schlesner, M. Complex heatmaps reveal patterns and correlations in
797 multidimensional genomic data. *Bioinformatics* **32**, 2847-2849,
798 doi:10.1093/bioinformatics/btw313 (2016).
799 76 Ma, C., Xin, M., Feldmann, K. A. & Wang, X. Machine learning-based differential network
800 analysis: a study of stress-responsive transcriptomes in Arabidopsis. *Plant Cell* **26**, 520-537,
801 doi:10.1105/tpc.113.121913 (2014).

77 Shannon, P. *et al.* Cytoscape: a software environment for integrated models of biomolecular interaction networks. *Genome Res* **13**, 2498-2504, doi:10.1101/gr.1239303 (2003).

78 Young, M. D., Wakefield, M. J., Smyth, G. K. & Oshlack, A. Gene ontology analysis for RNA-seq: accounting for selection bias. *Genome Biol* **11**, R14, doi:10.1186/gb-2010-11-2-r14 (2010).

79 Gotz, S. *et al.* High-throughput functional annotation and data mining with the Blast2GO suite. *Nucleic Acids Res* **36**, 3420-3435, doi:10.1093/nar/gkn176 (2008).

80 Yeom, S. I., Seo, E., Oh, S. K., Kim, K. W. & Choi, D. A common plant cell-wall protein HyPRP1 has dual roles as a positive regulator of cell death and a negative regulator of basal defense against pathogens. *Plant J* **69**, 755-768, doi:10.1111/j.1365-313X.2011.04828.x (2012).